

Carbazolyl Benzo[1,2-*b*:4,5-*b'*]difuran: An Ambipolar Host Material for Full-Color Organic Light-Emitting Diodes

Chikahiko Mitsui,^[a] Hayato Tsuji,^{*[a]} Yoshiharu Sato,^{*[b]} and Eiichi Nakamura^{*[a, b]}

Abstract: We have designed an ambipolar material, 3,7-bis[4-(*N*-carbazolyl)-phenyl]-2,6-diphenylbenzo[1,2-*b*:4,5-*b'*]difuran (CZBDF), and synthesized it by zinc-mediated double cyclization. Its physical properties clarified that CZBDF possesses a wide-gap character, well-balanced and high hole and electron mobilities of larger than

$10^{-3} \text{ cm}^2 \text{ V}^{-1} \text{ s}^{-1}$, and a high thermal stability. Using CZBDF as a host material for heterojunction OLED devices,

a full range of visible emission was obtained. Notably, CZBDF also enabled us to fabricate RGB-emitting homo-junction OLEDs, with performances comparable or superior to the heterojunction devices composed of several materials.

Keywords: ambipolar material • benzodifuran • host-guest system • organic light-emitting diodes • semiconductors

Introduction

Organic synthesis is playing a pivotal role in the development of functional π -conjugated materials^[1] for use in organic semiconducting devices, such as organic light-emitting diodes (OLEDs)^[2–4] for portable and flexible displays. Ambipolar organic semiconductors that transport both holes and electrons serve either as an emissive material or as a conductive host matrix in the emission layer.^[5] Considerations of both inter- and intramolecular interactions are mandatory for the design of efficient semiconductors. For a compound to act as a good semiconductor, the intermolecular orbital interaction should be maximized. For the compound to show ambipolarity, the installation of both p- and n-type moieties in one molecule is one possible strategy, in which each molecule can transfer both holes and electrons in opposite directions. In addition, for the ambipolar compound to be a versatile host in an emissive layer, it needs to have a wide HOMO/LUMO gap so that a single host material can be used for light emission from blue to red dopants.^[6] However, installation of donor and acceptor moieties in one molecule and its stacking in a macroscopic solid tends to

result in either intra- or intermolecular annihilation of the hole and electron pair rather than intermolecular carrier transport between two ends of a macroscopic solid because the latter is obviously intrinsically more difficult to achieve. Thus, an ideal ambipolar molecule must possess both high-HOMO donor and low-LUMO acceptor moieties that have no direct intramolecular π -conjugation with each other. We conjecture that any substituent that can transport an electron can be installed on a recently designed hole-transporting 2,6-phenylbenzo[1,2-*b*:4,5-*b'*]difuran (hereafter called BDF),^[7] without direct π -conjugation, by exploiting the steric congestion that will twist the added electron-transporting moiety(ies) away from the BDF core (Figure 1).

Herein, we report the design and synthesis of a new ambipolar material, 3,7-bis[4-(*N*-carbazolyl)phenyl]-2,6-diphenylbenzo[1,2-*b*:4,5-*b'*]difuran (CZBDF)^[7] possessing the following features: 1) well-balanced hole and electron mobilities in the order of $10^{-3} \text{ cm}^2 \text{ V}^{-1} \text{ s}^{-1}$ when amorphous; 2) a wide HOMO/LUMO gap with a value higher than 3 eV; and 3) deep-blue light emission, which allows the material to serve as a host for blue, green, and yellow fluorescent dopants as well as a red-phosphorescent dopant. We first de-

[a] Dr. C. Mitsui, Dr. H. Tsuji, Prof. Dr. E. Nakamura
Department of Chemistry
The University of Tokyo
Hongo, Bunkyo-ku, Tokyo 113-0033 (Japan)
Fax: (+81)3-5800-6889
E-mail: nakamura@chem.s.u-tokyo.ac.jp

[b] Dr. Y. Sato, Prof. Dr. E. Nakamura
Nakamura Functional Carbon Cluster Project, ERATO
Japan Science and Technology Agency
Hongo, Bunkyo-ku, Tokyo 113-0033 (Japan)
E-mail: ysato@chem.s.u-tokyo.ac.jp

Supporting information for this article is available on the WWW under <http://dx.doi.org/10.1002/asia.201200062>.

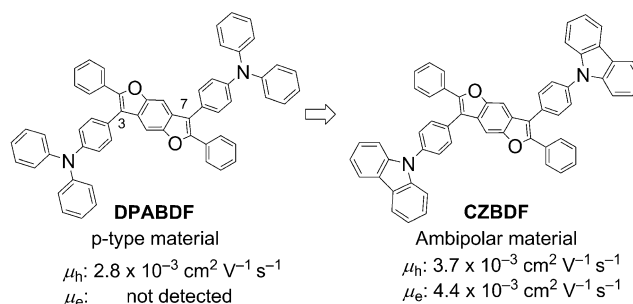


Figure 1. Structures and properties of BDF derivatives.

scribe its utility as a host matrix in the emission layer of a multilayer heterojunction OLED device,^[7] and then as a material for a homojunction OLED device that utilizes this compound as a single matrix of the whole organic layer. The latter device with a very simple architecture showed performances comparable with or superior to the state-of-the-art multilayer heterojunction devices, suggesting the feasibility of homojunction OLED devices for practical applications.

Results and Discussion

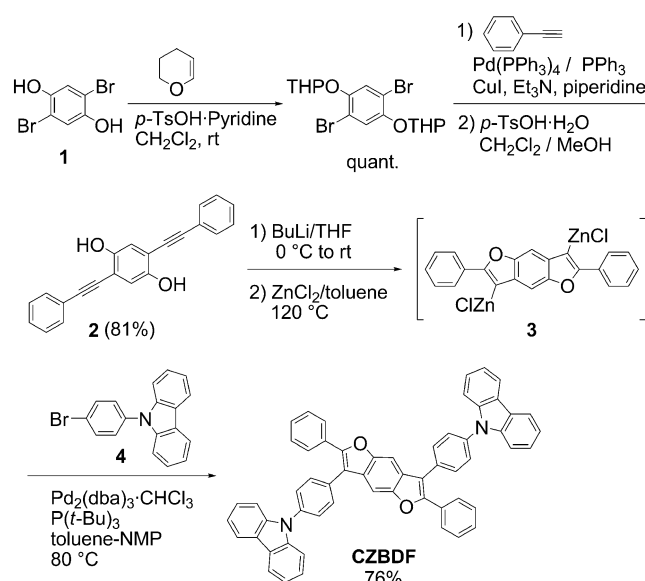
Molecular Design and Synthesis of CZBDF

The benzo[1,2-*b*:4,5-*b'*]difuran framework was recorded in the literature in the 19th century^[8] but has received little attention until we reported in 2007^[9] that its triphenylamine-substituted derivative (DPABDF) shows a high hole mobility ($\mu_h = 2.8 \times 10^{-3} \text{ cm}^2 \text{ V}^{-1} \text{ s}^{-1}$; yet undetectable electron mobility, μ_e), most probably because of the synergetic effect of the BDF core and the substituents, and serves as a useful hole-transporting material in OLEDs.^[10–13] The material has a wide band gap (optical gap: $\Delta E = 3.06 \text{ eV}$) due to the twisted orientation of the 3- and the 7-aromatic substituents against the BDF framework. This molecular structure inspired us to consider that installation of a proper group at 3- and 7-positions would create an ambipolar material having a wide HOMO/LUMO gap suitable for blue emission. We have chosen to install a carbazolyl group, which is a widely used motif to render an ambipolar property for a host material in OLEDs^[14] despite its inherent hole-transporting property. We thus synthesized CZBDF (Figure 1), expecting ambipolarity based on the synergetic effect between the BDF and carbazole moieties.^[15]

Synthesis of CZBDF has been performed by using a tandem zinc-mediated cyclization^[16]/cross-coupling reaction (Scheme 1), which makes a variety of BDF derivatives in a modular way^[17] using a 3,7-dizincio-BDF intermediate (**3**). Thus, 2,5-di(phenylethynyl)hydroquinone (**2**), which was obtained from commercially available 2,5-dibromo-1,4-hydroquinone (**1**) in three steps, was subjected to intramolecular double cyclization using zinc chloride at 120 °C to afford **3**, which was then coupled with *N*-(*p*-bromophenyl)carbazole (**4**) in the presence of a palladium catalyst^[18] using tritert-butylphosphine^[19] to obtain CZBDF in 76% isolated yield. The product was purified by repeated train sublimation for use in the following measurements and device applications.

Abstract in Japanese:

有機EL素子等の高効率化にむけて両極性材料に注目が集まっている。我々はカルバゾールを有するベンゾジフラン誘導体を合成し、物性を評価したところ、正孔・電子ともに $10^{-3} \text{ cm}^2/\text{Vs}$ 台の高い移動度を有することを見いだした。本材料を有機EL素子のホスト材料に応用することでフルカラー発光を示すヘテロ接合素子ならびに、ヘテロ接合素子と同等またはそれを凌駕する性能を示すホモ接合有機EL素子を実現した。



Scheme 1. Synthesis of CZBDF.

Properties of CZBDF

The wide-gap and ambipolar character of CZBDF was indicated by the electrochemical and photophysical measurements in solution. Cyclic voltammograms in CH_2Cl_2 and THF showed irreversible oxidation and reduction waves, respectively (Figure 2). Oxidation and reduction potentials determined by differential pulse voltammetry were 0.72 V (in CH_2Cl_2) and -2.60 V (in THF), respectively (vs Fc/Fc^+). The HOMO and LUMO energy levels (E_{HOMO} and E_{LUMO}) were estimated to be -5.52 eV and -2.20 eV , respectively, using the equation, E_{HOMO} or $E_{\text{LUMO}} = -(4.80 + E_{\text{DPV}})$. Thus, the HOMO/LUMO gap is 3.32 eV. This gap is wide enough

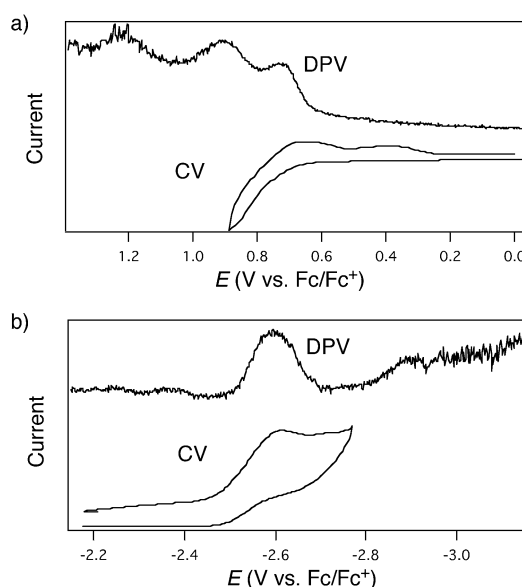


Figure 2. DPV (top) and CV (bottom) traces of CZBDF. Measurements were performed in CH_2Cl_2 (a) and THF (b) to determine oxidation and reduction potentials, respectively.

to confine carriers and excitons formed from common dopants for blue, green, yellow, and red colors (Figure 3), and suggests that CZBDF serves as a viable ambipolar material for OLEDs.

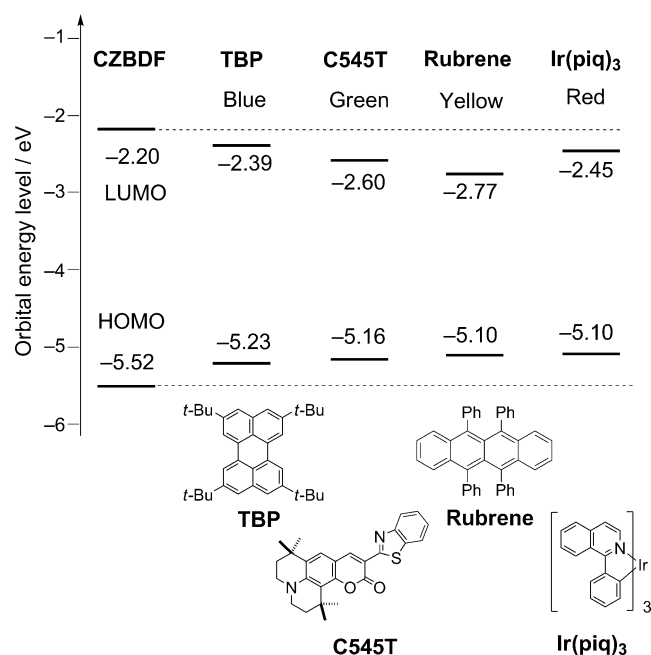


Figure 3. Orbital energy levels of host and dopants used in this study, together with the structures of dopants.

The UV/Vis absorption measurement in CH_2Cl_2 showed an absorption edge at 400 nm (Figure 4), and the optical gap (ΔE) was estimated to be 3.10 eV, which is close to that of DPABDF ($\Delta E=3.06$ eV), suggesting that the expected twisting inhibited the electronic interaction between the BDF core and the carbazole moieties. Upon photoexcitation

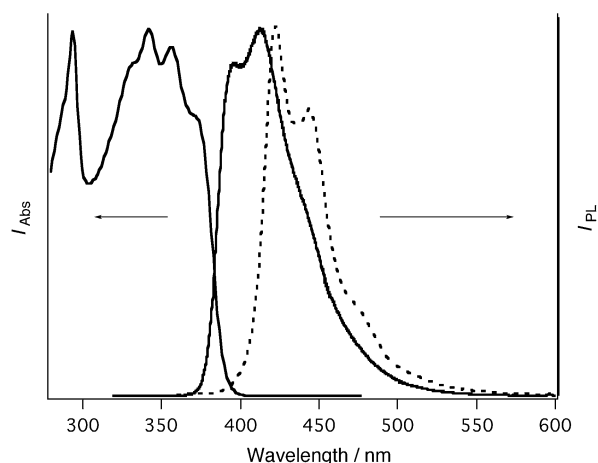


Figure 4. Absorption (left) and emission (right) spectra of CZBDF. Solid-line spectra were obtained in CH_2Cl_2 solution at room temperature. Dotted-line spectrum was obtained in powder form.

at 300 nm in CH_2Cl_2 , CZBDF emits deep-blue light with a maximum wavelength of 414 nm. The emission quantum yield was 0.97, as determined by the absolute method. The emission spectrum in the solid state was slightly red-shifted to 422 nm, thereby suggesting the presence of an intermolecular interaction. This agrees with the decrease of the emission quantum yield in the solid state to 0.61, a value still viable for an emissive material.

The thermal stability of CZBDF was unambiguously confirmed. Thermogravimetric analysis (TGA) showed that weight loss started at 450 °C and is less than 5% even at 500 °C, thus indicating that CZBDF will survive the vacuum deposition process used for device fabrication. The thermal stability of the amorphous state was evaluated by differential scanning calorimetry (DSC). An amorphous solid sample was obtained by the rapid cooling of a molten sample with liquid N_2 , and this was then subjected to DSC analysis at a heating rate of 10 K min^{-1} . The glass-transition temperature (T_g) of CZBDF (162 °C) is much higher than that of the most commonly used ambipolar material CBP (62 °C),^[20] which is beneficial for the longevity of the device.^[21]

Time-of-flight (TOF) carrier mobility was measured for an amorphous film of CZBDF (thickness: 3.3 μm) deposited under vacuum on a glass substrate coated with ITO. The transient photocurrent signals of both the hole and electron were dispersive. The carrier mobilities of CZBDF were plotted against the square root of the electric field (Figure 5). Hole and electron mobilities were 3.7×10^{-3} and $4.4 \times 10^{-3} \text{ cm}^2 \text{ V}^{-1} \text{ s}^{-1}$, respectively, in an electric field of $2.5 \times 10^5 \text{ V cm}^{-1}$ at room temperature. This level of well-balanced, high carrier mobilities rivals those reported for amorphous materials, and we consider that it originated from the cooperative effect of the BDF core and the carbazolyl groups.

Heterojunction OLED Devices

To investigate the viability of the new ambipolar material, we first examined the use of CZBDF as the host of the light

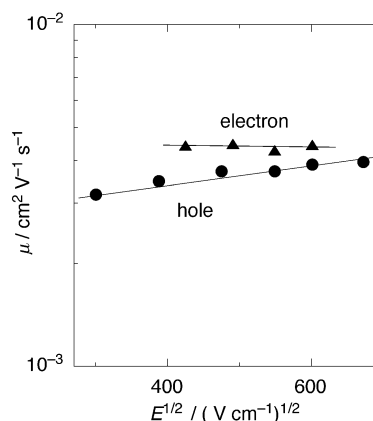


Figure 5. Hole and electron mobilities of CZBDF plotted against the square root of the electric field measured using the TOF method at room temperature employing a vacuum deposition film.

emission layer (EML) in heterojunction OLEDs. CZBDF was found to function by itself as a blue-emitting dye and to serve as a host material for various dopants over a full-color range. The device configurations of blue, green, and yellow OLEDs were ITO/MCC-PC1020^[22]/α-NPD^[1] (45 nm)/EML (emitting layer(s)) (30 nm)/Alq₃ (30 nm)/Liq (1 nm)/Al (as shown in Figure 6), where CZBDF was used in the EML

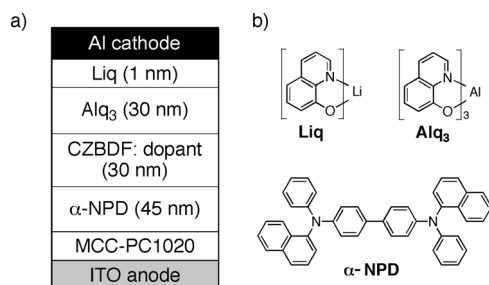


Figure 6. a) Heterojunction OLED structure of dye-doped devices. b) Structures of representative materials used in this study.

either as an emitting material by itself (undoped) or as a host material for various dopants (1–3 wt %). The structures of the dopants are shown in Figure 3. The electroluminescence (EL) spectra of the devices are shown in Figure 7. The device performances were evaluated with regard to three standard criteria: driving voltage (V_{1000}), maximum external quantum efficiency (EQE_{max}), and current efficiency (LJ_{1000}^{-1}), as summarized in Table 1.

The undoped device (device A) showed a deep-blue emission at 444 nm with Commission Internationale de l'Éclairage (CIE) coordinates of (0.177; 0.139). This emission can be assigned to that from CZBDF, but the maximum wavelength was slightly red-shifted when compared with the photoluminescence. No emission from any other material, such as Alq₃, was observed, indicating that efficient charge recombination takes place within the CZBDF layer. We next employed commercially available emissive dyes, the HOMO/LUMO levels of which were located between those of CZBDF, for an efficient carrier confinement within the emissive dopant molecules, leading to color tuning as well as enhanced EL performances. It was found that OLED devices using the dopants shown in Figure 3 show electrolumi-

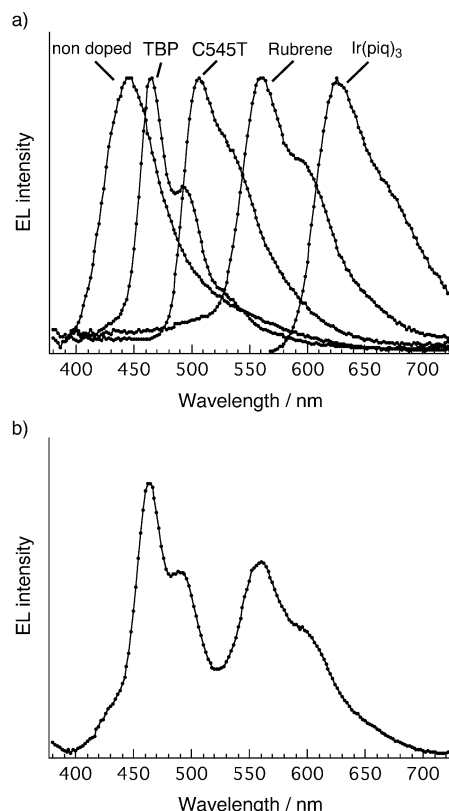


Figure 7. Electroluminescence spectra at 1000 cd m^{-2} of the OLED devices comprising CZBDF as an emissive material and a host material. a) Blue, green, yellow, and red emissive devices A–D and F. b) White emissive OLED device E.

nescence only from each dye, and not from the CZBDF host, indicating that the emissive dopants functioned as effectively as the recombination sites. The TBP (tetra-*tert*-butylperylene)-doped^[23] device (device B), for example, showed EL exclusively from the TBP dye with CIE coordinates of (0.160; 0.219), and the performance was higher than that of device A. Thus, device B showed a lower driving voltage ($V_{1000}=8.3 \text{ V}$ for device A vs. 6.7 V for device B) and higher external quantum efficiencies ($\text{EQE}_{\text{max}}=1.2\%$ for device A vs. 1.7% for device B) than device A. Similarly, C545T- (a coumarin-based dye)^[24] and rubrene-doped^[25] devices C and D showed green and yellow luminescence from

Table 1. Performances of OLEDs comprising either CZBDF or CBP in an emission layer.^[a]

Device	Host	Dopant	V_{1000} ^[b] [V]	EQE_{max} ^[c] [%]	LJ_{1000}^{-1} ^[d] [cd A^{-1}]	CIE coordinates ^[e]	
						x	y
A	CZBDF	None	8.3	1.2	1.2	0.177	0.139
B	CZBDF	TBP	6.7	1.7	1.9	0.160	0.219
C	CZBDF	C545T	6.2	2.7	5.3	0.269	0.570
D	CZBDF	rubrene	6.8	2.5	5.7	0.446	0.477
E	CZBDF	TBP and rubrene	7.4	1.8	3.2	0.304	0.325
F	CZBDF	Ir(piq) ₃	6.6	6.8	4.1	0.659	0.312
G	CBP	Ir(piq) ₃	9.1	6.4	5.4	0.653	0.317

[a] OLED performance data collected at a luminance of 1000 cd m^{-2} . [b] Driving voltage. [c] Maximum external quantum efficiency. [d] Current efficiency. [e] Commission Internationale de l'Éclairage coordinates.

each dopant with driving voltages of 6.2 V and 6.8 V and good external quantum efficiencies of 2.7% and 2.5%, respectively.

We next fabricated a white-emitting OLED by stacking a TBP-doped blue-emitting layer over the rubrene-doped yellow-emitting layer (device E). The device structure of this white OLED is as follows: ITO/MCC-PC1020/ α -NPD (45 nm)/1.7 wt% TBP-doped CZBDF (20 nm)/2.7% rubrene-doped CZBDF (10 nm)/Alq₃ (30 nm)/Liq (1 nm)/Al. The CIE coordinates of this device were (0.304; 0.325) at a luminance of 1,000 cd m⁻², which is close to the ideal white (0.333; 0.333). The CIE coordinates barely changed (less than 0.02) at a brightness in the range 200–47,000 cd m⁻², suggesting the steady and balanced charge recombination within both TBP- and rubrene-doped layers.

CZBDF was also applicable as the host material for a red-phosphorescent dye, Ir(piq)₃^[26] (device F). The structure of device F is ITO/MCC-PC1020/ α -NPD (45 nm)/CZBDF: 4.0 wt% Ir(piq)₃ (30 nm)/BCP (10 nm)/Alq₃ (20 nm)/Liq (1 nm)/Al, in which BCP (2,9-dimethyl-4,7-diphenyl-9,10-phenanthroline) was used as hole- and exciton-blocking material to confine carrier and triplet excitons within the emissive layer. Device F showed an external quantum efficiency of 6.8%, which is higher than the theoretical limit for a fluorescent OLED device (ca. 5%).^[27] The performance of this device was superior to that of an OLED device using CBP (*N,N'*-dicarbazolyl-4,4'-biphenyl), a commonly used host material (device G). The external quantum efficiency of device F was higher than that of device G (6.4%), with a significant improvement in the driving voltage (6.6 V for device F and 9.1 V for device G). The lifetime of device F was also much longer (4,250 h) than device G (260 h), as measured using a constant current mode (at 12.5 mA cm⁻², Figure 8). The long lifetime of CZBDF-based devices can be attributed to the stable amorphicity of CZBDF and its lower driving voltage due to a suitable HOMO/LUMO energy level for neighboring layers and a high CZBDF carrier mobility. Further optimization of the CZBDF-based structure will prolong the lifetime of such a device for practical use.

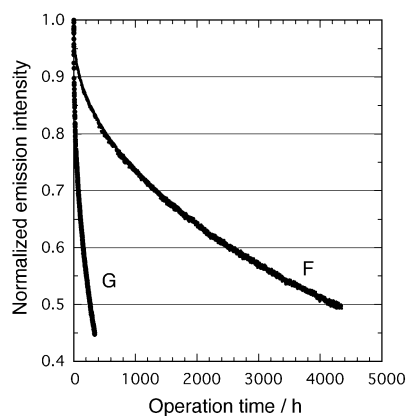


Figure 8. Operation-lifetime measurement for devices F and G.

Homojunction OLED Devices

With promising results from the heterojunction devices in hand, we next examined the use of CZBDF in a homojunction setting, as it offers a much simpler architecture than the popular heterojunction device (see, for example, Figure 6a). While such a homojunction architecture was previously studied for organic photovoltaic devices by Leo et al.,^[28–30] it has seldom been reported in OLED research except for a report in a conference proceeding,^[31] and some studies^[32] that were published following our original communication.^[7] This is clearly because of the paucity of suitable ambipolar materials. First, the diode properties of two types of CZBDF-based homojunction devices were examined: a single-layer device using only CZBDF (Figure 9a, or device H in Table 2) and a p/n-doped homojunction device,

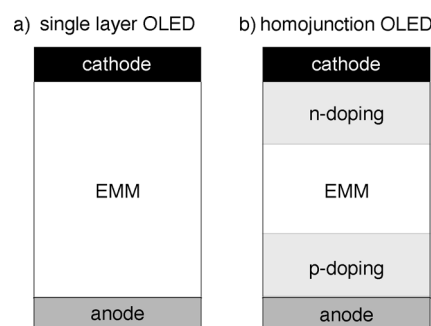


Figure 9. Schematic device structures of the OLEDs. a) Single-layer device (device H) and b) p-i-n homojunction device (devices I–L).

in which vanadium oxide (V₂O₅, p-dopant) and cesium (Cs, n-dopant) were respectively doped on the bottom and top parts in the device by co-deposition under vacuum (Figure 9b or device I). As shown in Figure 10a, the current density-voltage (*J*–*V*) characteristics indicate that only the p/n-doped device I showed a good diode character (on/off ratio: ca. 10³ and turn-on voltage: ca. 1 V), while device H did not. Thus, the inorganic p/n-doping endows the homogeneous CZBDF layer with diode characteristics by facilitating carrier generation and injection from the electrodes to the organic layer.^[33,34] The p/n-doping device I also increases the efficiency of charge recombination in the CZBDF layer, and thus device I had a deep-blue emission that peaked at 428 nm (Figure 10b) with an EQE_{max} of 0.5% at 4 V. The emission maximum wavelength is close to that obtained by photoluminescence (422 nm), while blue shifted when compared with the corresponding heterojunction device A (444 nm). We conjecture that this shift in the heterojunction device was a result of the filtering effect caused by layers other than the emission layer.

We next examined the performance of various emissive dyes in a p-i-n homojunction device using CZBDF, where we doped the i-layer by co-deposition of a dye dopant and CZBDF (matrix), and achieved full-color emission in the homojunction architecture. We chose blue-fluorescent TBP,

Table 2. Summary of the OLED structures studied and their characteristics.

Device	Device structure	p/n-doping ^[a]	Emissive dopant	Emission color	λ_{\max} ^[b] [nm]	L_{\max} ^[c] [cd m^{-2}]	EQE_{\max} ^[d] [%]
H	7a	–	None	NA ^[e]	NA ^[e]	NA ^[e]	NA ^[e]
I	7b	+	None	Blue	428	1,170	0.5
J	7b	+	TBP	Blue	464	10,200	1.0
K	7b	+	C545T	Green	506	60,590 ^[f]	4.2 ^[g]
L	7b	+	Ir(piq) ₃	Red	628	4,690	5.6 ^[h]

[a] p-dopant = V_2O_5 , n-dopant = Cs. [b] Emission maximum wavelength in nanometers at a luminance of 1000 cd m^{-2} . [c] Maximum luminance. [d] Maximum external quantum efficiency. [e] Not available because the maximum luminance did not reach 1000 cd m^{-2} . [f] At 14 V. [g] At 13 V. [h] At 10 V.

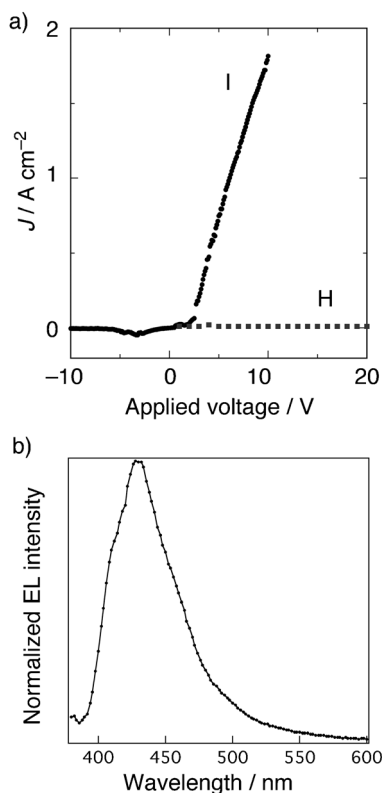


Figure 10. a) Diode characteristics of the single-layer device H (without doping) and the p/n-doped device I. b) EL spectrum of device I.

green-fluorescent C545T, and red-phosphorescent material, Ir(piq)₃, the same dopants as for the heterojunction devices. The configuration of the homojunction devices (devices J–L) was ITO/CZBDF: V_2O_5 (30 nm)/CZBDF:(emissive dopant)/CZBDF:Cs (20 nm)/Al, where emissive dopants were introduced by co-deposition with CZBDF under vacuum. The thickness of the emissive layer was 50 nm for device J and 100 nm for devices K and L. The dye-doped devices showed electroluminescence from the dopants, and no light emission was observed from the CZBDF host, indicating that the emissive dopants functioned very well as the recombination sites. The L – V characteristics and EQE values of devices J–L are plotted against the applied voltage in Figure 11. Devices J–L showed much better efficiencies than device I (Table 2). Remarkably, the homojunction devices J–L displayed a similar, and sometimes even better performance than the corresponding heterojunction devices (devices B, C, and F). With regard to the blue-fluorescent TBP-

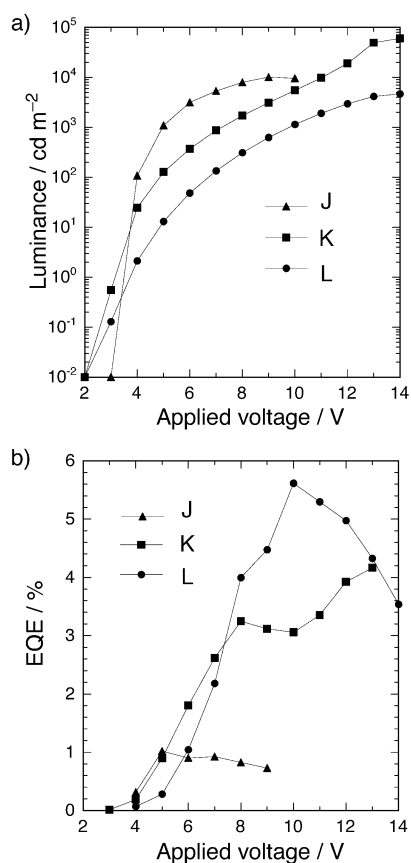


Figure 11. EL characteristics for p-i-n homojunction devices (devices J–L) using CZBDF as a host matrix. a) L – V characteristics. b) Plot of EQE against applied voltage.

doped devices, the homojunction device J drove at a lower voltage than the heterojunction device B ($V_{1000}=4.9 \text{ V}$ for device J vs. 6.7 V for device B); however, the EQE were somewhat low ($\text{EQE}_{\max}=1.0\%$ for device J vs. 1.7% for device B). The green-fluorescent C545T-doped homojunction device K achieved a high EQE_{\max} value of 4.2% at a luminance higher than $60\,000 \text{ cd m}^{-2}$, while the corresponding heterojunction device C reached only 2.7% . The high EQE value is close to the theoretical limit of a fluorescent OLED (ca. 5%).

The p-i-n homojunction architecture was also effective in a red-phosphorescent OLED. The Ir(piq)₃-doped device L gave an EQE_{\max} value of 5.6% , which is higher than the theoretical limit for a fluorescent OLED device. However, this

$E_{QE_{max}}$ value was somewhat lower than that of the six-layer heterojunction device F with a hole- and exciton-blocking BCP layer (6.8%).

Conclusions

We have developed a new ambipolar material, CZBDF, composed of a BDF skeleton and two carbazole moieties connected to each other through twisted C–C bonds. CZBDF possesses well-balanced hole and electron mobilities of greater than $10^{-3} \text{ cm}^2 \text{ V}^{-1} \text{ s}^{-1}$. The carrier mobilities are higher than BDF (hole mobility) or CBP (electron mobility) alone, which we consider is due to the twisted molecular structure that may have resulted in intertwinning and larger interactions between the molecular orbitals than for BDF and CBP alone; however, we have not been able to obtain crystal structures to confirm this assumption. CZBDF has a wide HOMO/LUMO gap of $>3.3 \text{ eV}$, and serves as a deep-blue emissive material as well as an effective emission host material for various dopants emitting over the full range of visible light. A CZBDF-based device shows better performance and a much longer lifetime than the widely examined CBP-based device. These useful properties of CZBDF allowed us to develop full-color emissive p-i-n homojunction OLEDs, which performed at a level similar to, or higher than, the structurally more complex heterojunction devices made from several material combinations. Although homojunction devices using a single ambipolar material are attractive because of their structural simplicity, they require much more stringent materials design than heterojunction devices in which the properties of the unipolar material for each layer can be optimized pertaining to the specific function of each layer. The BDF-based homojunction devices reported here illustrate the feasibility of a high-performance homojunction OLED enabled by the development of suitable ambipolar materials.

Experimental Section

Synthesis of CZBDF

To a suspension of 2,5-bis(phenylethynyl)-1,4-benzenediol (124 mg, 0.400 mmol) in THF (0.8 mL) was added a solution of *n*-butyllithium in hexane (0.48 mL, 1.66 mol L^{-1} , 0.80 mmol) at 0°C . The resulting yellow suspension was allowed to warm to ambient temperature and stirred for 30 min. A solution of zinc chloride in THF (0.80 mL, 1.0 mol L^{-1} , 0.80 mmol) was then added. Subsequently, the volatiles were removed in vacuo and toluene (0.8 mL) was added. The resulting yellow solution was heated to 120°C and stirred for 2.5 h at this temperature. After cooling to ambient temperature, *N*-methylpyrrolidone (NMP) (0.2 mL), $\text{Pd}_2(\text{dba})_3\text{CHCl}_3$ (41.4 mg, 0.04 mmol), $\text{P}(\text{tBu})_3$ in toluene (160 μL , 1.0 mol L^{-1} , 0.16 mmol), and 4-bromophenylcarbazole (309 mg, 0.960 mmol) were successively added. The resulting mixture was stirred for 25 h at 80°C . After cooling to ambient temperature, the precipitate was collected by filtration and washed several times with MeOH and EtOAc. The resulting crude solid product was purified by gradient vacuum sublimation (pressure $<20 \text{ mTorr}$) at $380\text{--}400^\circ\text{C}$ to obtain the title compound (193 mg, 61%) as a white powder. A second crop was obtained from the mother liquor. After removal of the solvent in vacuo, the

combined organic layers were passed through a silica gel column employing CHCl_3 as the eluent. After removal of the solvent in vacuo, the crude material was purified by gel permeation chromatography to afford the title compound (48 mg, 15%). Hence, the total yield was 76%. $^1\text{H NMR}$ (500 MHz, 1,2-dideutero-1,1,2,2-tetrachloroethane): $\delta = 7.29\text{--}7.34$ (m, 6H, carbazole and p-Ph), 7.37 (dd, $J = 7.4 \text{ Hz}$, 7.4 Hz, 4H, *m*-Ph), 7.46 (dd, $J = 8.1 \text{ Hz}$, 8.1 Hz, 4H, carbazole), 7.57 (d, $J = 8.1 \text{ Hz}$, 4H, carbazole), 7.70–7.76 (m, 10H, benzodifuran, phenylene, and *o*-Ph), 7.79 (d, $J = 8.0 \text{ Hz}$, 4H, phenylene), 8.14 ppm (d, $J = 8.1 \text{ Hz}$, 4H, carbazole); $^{13}\text{C NMR}$ (125 MHz, 1,2-dideutero-1,1,2,2-tetrachloroethane at 100°C): $\delta = 101.0, 110.0, 117.2, 120.3, 120.4, 123.8, 126.2, 127.2, 127.6, 128.6, 128.7, 129.2, 130.7, 131.4, 132.3, 137.5, 141.1, 151.7, 152.2$ ppm; IR (solid): $\tilde{\nu} = 3046$ (w), 1594 (m), 1521 (m), 1490 (m), 1451 (s), 1227 (s), 1146 (m), 1061 (m), 957 (m), 749 cm^{-1} (s); MS (APCI+): 793 [M^+]; elemental analysis calcd. (%) for $\text{C}_{58}\text{H}_{36}\text{N}_2\text{O}_2$: C 87.86; H 4.58, N 3.53; found: C 87.97, H 4.71, N 3.45.

General

UV/Vis absorption spectra were recorded with a JASCO V-570 spectrometer at a resolution of 0.5 nm. Spectroscopy-grade dichloromethane was used as a solvent. Sample solutions (ca. 10 μM) in a 1 cm square quartz cell were used for the measurements. Photoluminescence spectra (PL) and absolute quantum yields were recorded with a Hamamatsu Photonics C9920-02 Absolute PL Quantum Yield Measurement System. Degassed spectroscopy-grade dichloromethane was used as a solvent. All measurements were performed at room temperature.

Cyclic voltammetry (CV) was performed using a HOKUTO DENKO HZ-5000 voltammetric analyzer. A glassy carbon electrode was used as the working electrode, a platinum coil as the counter electrode, and Ag^+/Ag as the reference electrode, at a scan rate of 100 mV s^{-1} . The compound was dissolved in degassed, dry CH_2Cl_2 and THF at a concentration of ca. 5 mM, and tetrabutylammonium perchlorate at a concentration of 0.1 M was added as an electrolyte. All potentials were determined by differential pulse voltammetry (DPV), and were corrected from a ferrocene standard.

Thermogravimetric analysis (TGA) was performed on a Rigaku Thermo Plus 2 instrument. The samples ($\sim 5 \text{ mg}$) were placed in aluminum pans and heated at 10 K min^{-1} under N_2 gas at a flow rate of 100 mL min^{-1} .

Differential scanning calorimetry (DSC) was performed on a NETZSCH thermal analyzer (DSC 204/F1). An amorphous sample was obtained by fast cooling the melt of CZBDF, and the obtained sample was heated at a rate of 10 K min^{-1} under N_2 gas, at a flow rate of 18 mL min^{-1} .

The time-of-flight (TOF) measurement was performed using a TOF-401 instrument (Sumitomo Heavy Industries Advanced Machinery). Films were deposited on indium tin oxide (ITO, 145 nm)-coated glass substrates. The vacuum deposition was performed using a VPC-260 system (ULVAC KIKO). The films were deposited by vacuum sublimation at $1 \times 10^{-3} \text{ Pa}$, with an average deposition rate of $20\text{--}30 \text{ nm s}^{-1}$. The ITO-coated glass substrate was spaced at 100 mm from the sample, and it was kept at 25°C . The thickness of the films obtained was 3.3 μm .

For the device fabrication and evaluation, CZBDF with analytical purity was purified further by train sublimation. All other materials were used as obtained commercially. An ITO-coated glass substrate treated by O_3 -plasma was used as the anode. For the fabrication of heterojunction OLED devices, MCC-PC1020 was spin-coated onto this substrate, dried, and annealed at 230°C under nitrogen atmosphere. All other layers were vacuum deposited onto this substrate at a pressure of $2 \times 10^{-4} \text{ Pa}$ or less. Finally, the device was sealed by encapsulation with a fresh desiccant under nitrogen atmosphere. The emissive area of the device was $2 \times 2 \text{ mm}^2$.

Acknowledgements

We thank MEXT (KAKENHI for E.N., No. 22000008, H.T., No. 20685005) and the Global COE Program for Chemistry Innovation. C.M.

thanks the Research Fellowship of the Japan Society for the Promotion of Science for Young Scientists (No. 219262).

- [1] For hole-transporting materials, see: a) S. A. Van Slyke, C. H. Chen, C. W. Tang, *Appl. Phys. Lett.* **1996**, *69*, 2160; b) M. Thelakkat, H. W. Schmidt, *Adv. Mater.* **1998**, *10*, 219; c) K. Katsuma, Y. Shirota, *Adv. Mater.* **1998**, *10*, 223. For electron-transporting materials, see: d) S. J. Su, Y. Takahashi, T. Chiba, T. Takeda, J. Kido, *Adv. Funct. Mater.* **2009**, *19*, 1260; e) M. Ichikawa, S. Fujimoto, Y. Miyazawa, T. Koyama, N. Yokoyama, T. Miki, Y. Taniguchi, *Org. Electron.* **2008**, *9*, 77.
- [2] C. W. Tang, S. A. VanSlyke, *Appl. Phys. Lett.* **1987**, *51*, 913.
- [3] a) K. Müllen, U. Scherf, *Organic Light-Emitting Devices: Synthesis Properties and Applications*, Wiley-VCH, Weinheim, **2006**; b) *Organic Light-Emitting Devices: A Survey* (Ed.: J. Shinar), Springer, New York, **2004**; c) Z. Li, H. Meng, *Organic Light-Emitting Materials and Devices*, CRC Press, Boca Raton, **2007**.
- [4] C. Adachi, T. Tsutsui, in *Organic Light-Emitting Devices: A Survey* (Ed.: J. Shinar), Springer, New York, **2004**, pp. 43–69.
- [5] For a review of bipolar materials, see: A. Chaskar, H. F. Chen, K. T. Wong, *Adv. Mater.* **2011**, *23*, 3876.
- [6] C.-L. Ho, L.-C. Chi, W.-Y. Hung, W.-J. Chen, Y.-C. Lin, H. Wu, E. Mondal, G.-J. Zhou, K.-T. Wong, W.-Y. Wong, *J. Mater. Chem.* **2012**, *22*, 215.
- [7] CZBDF-based homojunction devices have been communicated: H. Tsuji, C. Mitsui, Y. Sato, E. Nakamura, *Adv. Mater.* **2009**, *21*, 3776.
- [8] F. R. Japp, A. N. Meldrum, *J. Chem. Soc.* **1899**, *75*, 1035.
- [9] H. Tsuji, C. Mitsui, L. Ilies, Y. Sato, E. Nakamura, *J. Am. Chem. Soc.* **2007**, *129*, 11902.
- [10] For a study on bioactivity, see: J. J. Chambers, D. M. Kurrasch-Orbaugh, M. A. Parker, D. E. Nichols, *J. Med. Chem.* **2001**, *44*, 1003.
- [11] For recent synthetic examples, see: a) J. C. González-Gómez, L. Santana, E. Uriarte, *Tetrahedron* **2005**, *61*, 4805; b) D. Yue, T. Yao, R. C. Larock, *J. Org. Chem.* **2005**, *70*, 10292; c) Z. Liang, S. Ma, J. Yu, R. Xu, *J. Org. Chem.* **2007**, *72*, 9219; d) Y. Matsuura, Y. Tanaka, M. Akita, *J. Organomet. Chem.* **2009**, *694*, 1840; e) K. Tsuchikama, Y.-k. Hashimoto, K. Endo, T. Shibata, *Adv. Synth. Catal.* **2009**, *351*, 2850; f) C. Yi, C. Blum, M. Lehmann, S. Keller, S.-X. Liu, G. Frei, A. Neels, J. Hauser, S. Schürch, S. Decurtins, *J. Org. Chem.* **2010**, *75*, 3350; g) R. M. Gay, F. Manarin, C. C. Schneider, D. A. Barancelli, M. D. Costa, G. Zeni, *J. Org. Chem.* **2010**, *75*, 5701.
- [12] For studies on properties, see: a) R. Shukla, S. H. Wadumethrige, S. V. Lindeman, R. Rathore, *Org. Lett.* **2008**, *10*, 3587; b) N. Hayashi, Y. Saito, H. Higuchi, K. Suzuki, *J. Phys. Chem. A* **2009**, *113*, 5342.
- [13] An example of a device application with benzodifuran derivatives has been presented in: H. Li, P. Jiang, C. Yi, C. Li, S.-X. Liu, S. Tan, B. Zhao, J. Braun, W. Meier, T. Wandlowski, S. Decurtin, *Macromolecules* **2010**, *43*, 8058.
- [14] a) D. F. O'Brien, M. A. Baldo, M. E. Thompson, S. R. Forrest, *Appl. Phys. Lett.* **1999**, *74*, 442; b) M. A. Baldo, S. Lamansky, P. E. Burrows, M. E. Thompson, S. R. Forrest, *Appl. Phys. Lett.* **1999**, *75*, 4.
- [15] Molecular orbital calculations at the B3LYP/6-31G* level show that HOMO and LUMO of CZBDF are located mostly within the BDF moiety, thus suggesting that the BDF moiety contributes to the carrier transportation. Since tetraphenyl-BDF (TPBDF) does not show any electron-transporting ability as discussed in Ref. [9], we consider that the installation of the carbazole moiety renders the electron-transporting ability to CABDF (see the Supporting Information).
- [16] a) M. Nakamura, L. Ilies, S. Otsubo, E. Nakamura, *Angew. Chem.* **2006**, *118*, 958; *Angew. Chem. Int. Ed.* **2006**, *45*, 944; b) M. Nakamura, L. Ilies, S. Otsubo, E. Nakamura, *Org. Lett.* **2006**, *8*, 2803.
- [17] a) H. Tsuji, K. Sato, L. Ilies, Y. Itoh, Y. Sato, E. Nakamura, *Org. Lett.* **2008**, *10*, 2263; b) L. Ilies, H. Tsuji, Y. Sato, E. Nakamura, *J. Am. Chem. Soc.* **2008**, *130*, 4240; c) H. Tsuji, Y. Yokoi, C. Mitsui, L. Ilies, Y. Sato, E. Nakamura, *Chem. Asian J.* **2009**, *4*, 655; d) H. Tsuji, K. Sato, Y. Sato, E. Nakamura, *J. Mater. Chem.* **2009**, *19*, 3364; e) H. Tsuji, K. Sato, Y. Sato, E. Nakamura, *Chem. Asian J.* **2010**, *5*, 1294; f) L. Ilies, Y. Sato, C. Mitsui, H. Tsuji, E. Nakamura, *Chem. Asian J.* **2010**, *5*, 1376; g) H. Tsuji, C. Mitsui, Y. Sato, E. Nakamura, *Heteroat. Chem.* **2011**, *22*, 316; h) H. Tsuji, G. M. O. Favier, C. Mitsui, S. Lee, D. Hashizume, E. Nakamura, *Chem. Lett.* **2011**, *40*, 576; i) C. Mitsui, H. Tanaka, H. Tsuji, E. Nakamura, *Chem. Asian J.* **2011**, *6*, 2296.
- [18] a) E. Negishi, A. O. King, N. Okukado, *J. Org. Chem.* **1977**, *42*, 1821; b) E. Negishi, T. Takahashi, A. O. King, *Org. Synth.* **1985**, *66*, 67.
- [19] a) T. Yamamoto, M. Nishiyama, Y. Koie, *Tetrahedron Lett.* **1998**, *39*, 2367; b) C. Dai, G. C. Fu, *J. Am. Chem. Soc.* **2001**, *123*, 2719; c) G. C. Fu, *Acc. Chem. Res.* **2008**, *41*, 1555.
- [20] M. H. Tsai, Y. H. Hong, C. H. Chang, H. C. Su, C. C. Wu, A. Mato-liukstyte, J. Simokaitiene, S. Grigalevicius, J. V. Grazulevicius, C. P. Hsu, *Adv. Mater.* **2007**, *19*, 862.
- [21] B. W. D'Andrade, S. R. Forrest, A. B. Chwang, *Appl. Phys. Lett.* **2003**, *83*, 3858.
- [22] S. J. Su, E. Gonmori, H. Sasabe, J. Kido, *Adv. Mater.* **2008**, *20*, 4189.
- [23] B. X. Mi, Z. Q. Gao, C. S. Lee, S. T. Lee, H. L. Kwong, N. B. Wong, *Appl. Phys. Lett.* **1999**, *75*, 4055.
- [24] C. H. Chen, C. W. Tang, *Appl. Phys. Lett.* **2001**, *79*, 3711.
- [25] M. S. Jang, S. Y. Song, H. K. Shim, T. Zyung, S. D. Jung, L.-M. Do, *Synth. Met.* **1997**, *91*, 317.
- [26] A. Tsuboyama, H. Iwakaki, M. Furugori, T. Mukaide, J. Kamatani, S. Igawa, T. Moriyama, S. Miura, T. Takiguchi, S. Okada, M. Hoshino, K. Ueno, *J. Am. Chem. Soc.* **2003**, *125*, 12971.
- [27] N. C. Greenham, R. H. Friend, D. D. C. Bradley, *Adv. Mater.* **1994**, *6*, 491.
- [28] K. Walzer, B. Maennig, M. Pfeiffer, K. Leo, *Chem. Rev.* **2007**, *107*, 1233.
- [29] K. Harada, A. G. Werner, M. Pfeiffer, C. J. Bloom, C. M. Elliott, K. Leo, *Phys. Rev. Lett.* **2005**, *94*, 036601.
- [30] K. Harada, M. Riede, K. Leo, O. R. Hild, C. M. Elliott, *Phys. Rev. B* **2008**, *77*, 195212.
- [31] T. Mori, A. Oda, J. Kido, *Proceedings of The Japan Society of Applied Physics and Related Societies* **2006**, *53*, 1395.
- [32] a) C. Cai, S. J. Su, T. Chiba, H. Sasabe, Y. J. Pu, K. Nakayama, J. Kido, *Jpn. J. Appl. Phys.* **2011**, *50*, 040204; b) C. Cai, S. J. Su, T. Chiba, H. Sasabe, Y. J. Pu, K. Nakayama, J. Kido, *Org. Electron.* **2011**, *12*, 843; c) S. Hamwi, T. Riedl, W. Kowalsky, *Appl. Phys. Lett.* **2011**, *99*, 053301; d) Q. Wang, Y. Tao, X. Qiao, J. Chen, D. Ma, C. Yang, J. Qin, *Adv. Funct. Mater.* **2011**, *21*, 1681; e) X. Qiao, Y. Tao, Q. Wang, D. Ma, C. Yang, L. Wang, J. Qin, F. Wang, *J. Appl. Phys.* **2010**, *108*, 034508.
- [33] J. Endo, T. Matsumoto, J. Kido, *Jpn. J. Appl. Phys.* **2002**, *41*, L358.
- [34] Y. Kishigami, K. Tsubaki, Y. Kondo, J. Kido, *Synth. Met.* **2005**, *153*, 241.

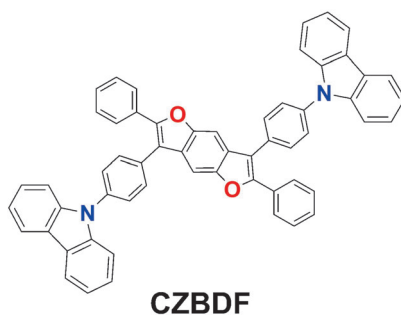
Received: January 18, 2012

Revised: February 27, 2012

Published online: ■■■, 0000

FULL PAPERS

The (Ambi)Polar Express: A newly designed ambipolar material, CZBDF, was synthesized. CZBDF possesses a wide-gap character, well-balanced and high hole and electron mobilities of larger than $10^{-3} \text{ cm}^2 \text{ V}^{-1} \text{ s}^{-1}$, and a high thermal stability. This material functions as an emissive material and a host material for OLEDs and enabled us to produce heterojunction as well as p-i-n homojunction OLED devices that emit full-color visible light with high efficiency.



Organic Light-Emitting Diodes

Chikahiko Mitsui, Hayato Tsuji,*
Yoshiharu Sato,*
Eiichi Nakamura* ————— ■■■■-■■■■

Carbazoyl Benzo[1,2-*b*:4,5-*b'*]difuran: 
**An Ambipolar Host Material for Full-
Color Organic Light-Emitting Diodes**